Tetra-(p-tolyl)antimony(III)-Containing Heteropolytungstates, [(p-tolyl)SbIII4(A-α-XW9O34)2]n- (X = P, As, or Ge): Synthesis, Structure, and Study of Antibacterial and Antitumor Activity

Edit Trace of Manuscript 10.1021/acs.inorgchem.9b03322

Tetra--(*p*--tolyl)antimony(III)-containingContaining Heteropolytungstates, [{(*p*-tolyl-Tolyl)Sb^{III}}$_4$(*A*--α-XW_9O_{34})$_2$]$^{n-}$ (X = P, As, or Ge): Synthesis, Structure, and Study of Antibacterial/ and Antitumor Activity

Tian **Ma** ,[a†] Peng **Yang** ,[a†] Inga **Dammann** ,[a†] Zhengguo **Lin** ,[a†] Ali S. **Mougharbel** ,[a†] Ming-Xing **Li** ,[b‡] Florin **AdăsceăliţeiAdăscăliţei** ,[c§] Raluca **Mitea** ,[c§] Cristian **Silvestru** ,[c§] Candice **Thorstenson** ,[a†] Matthias S. **Ullrich** ,[a†] Klaudia **Cseh** ,[d∥] Michael A. **Jakupec** ,[d∥] Bernhard K. **Keppler** ,[d∥] Manuela **Donalisio** ,[e⊥] Roberta **Cavalli** ,[f#] David **Lembo** ,[e⊥] **and** Ulrich **Kortz** *,[a†]

[a†] **Department of Life Sciences and Chemistry**, **Jacobs University** , 28759 Bremen, Germany

[b‡] **Department of Chemistry, College of Sciences**, **Shanghai University** , Shanghai 200444, P.R.P. R. China

[c§] **Department of Chemistry, Supramolecular Organic and Organometallic Chemistry Centre (SOOMCC), Faculty of Chemistry and Chemical Engineering**, **BabeBabeş-Bolyai University** , 400028 Cluj-Napoca, Romania

[d∥] **Institute of Inorganic Chemistry, Faculty of Chemistry**, **University of Vienna** , 1090 Vienna, Austria

[e⊥] **Department of Clinical and Biological Sciences**, **University of Turin** , 10043 Orbassano (, Turin), Italy

[f#] **Department of Drug Science and Technology**, **University of Turin** , 10125 Turin, Italy

* U.K.: eE-mail: u.kortz@jacobs-university.de ; fax. Fax: +49 421 200 3102 ; tel. Telephone: +49 421 200 3235.

We have synthesized and structurally characterized three tetra-(*p*-tolyl)antimony(III)-containing heteropolytungstates, [{(*p*-tolyl)Sb^{III}}$_4$(*A*-α-XW_9O_{34})$_2$]$^{n-}$ ([X = P^V (**1-P**), As^V (**1-As**), or Ge^{IV} (**1-Ge**))], in aqueous solution using conventional, one-pot procedures. The polyanions **1-P**, **1-As**, and **1-Ge** were fully characterized in the solid state and in solution and were shown to be soluble and stable in aqueous medium at pH 7. Biological studies showed that all three polyanions display significant antibacterial and antitumor activities. The minimum inhibitory concentration (MIC)concentrations of **1-P**, **1-As**, and **1-Ge** were determined against four kinds of bacteria, including the two pathogenic bacteria strains, *Vibrio parahaemolyticusparahemolyticus* and *V.Vibrio vulnificus*. The three novel polyanions also showed high cytotoxic potency in the human cell lines A549 (non-small cell lung cancer), CH1/PA-1 (ovarian teratocarcinoma), and SW480 (colon carcinoma).

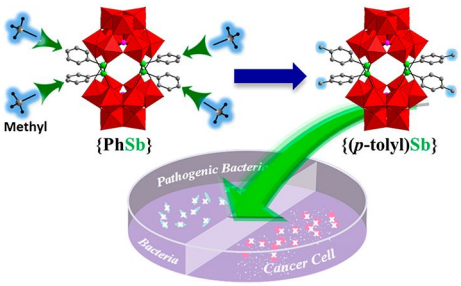

. Abstract Graphic

We have synthesized three tetra-(*p*-tolyl)antimony(III)-containing heteropolytungstates, [{(*p*-tolyl)Sb^{III}}$_4$(*A*-α-XW_9O_{34})$_2$]$^{n-}$ ([X = P (**1-P**), As (**1-As**), or Ge (**1-Ge**))], which were characterized in the solid state and in solution by a multitude of analytical techniques. The biological assays demonstrated antibacterial

activities of the novel polyanions and a higher antiproliferative activity against tumor cells than human foreskin fibroblasts.

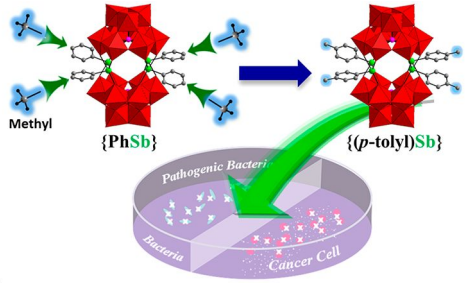

. TOC Graphic

Keywords: Polyoxometalates; organometallic chemistry; antimony; antibacterial; anticancer

1965371196537219653 73

SI File: ic9b03322_si_001.pdf

INTRODUCTIONIntroduction

Polyoxometalates (POMs) are discrete, polynuclear metal oxides with enormous structural and compositional variety, and a multitude of properties whichthat are of interest in fundamental and applied science.[1] The incorporation of organometallic moieties such as organophosphorus(V),[2] organosilicon(IV),[3] organogermanium(IV),[4] organoruthenium(II),[5] and organotin(IV),[6] in lacunary (vacant) heteropolytungstates may allow the modification of the shape, size, lipophilicity, solubility, stability, toxicity as well as, and redox and acid−base properties of POMs. Furthermore, from a biomedical point of view, it is possible to tune POMs for antimicrobial, antiviral, and antitumor properties, as well as protein crystallography.[7]

Organoantimony compounds, which are known to possess properties relevant for the fields of catalysis[8] and biology[9] (albeit less than organotin compounds), are usually synthesized by the self-condensation of arylstibonic acid.[10] In recent years, our group has developed thea class of organoantimony-containing POMs, and it was demonstrated that these compoundsthese compounds were shown to exhibit structure-dependent antibacterial activity. In 2012, the discrete phenylantimony(III)-containing heteropolytungstates $[(PhSb^{III})_4(A\text{-}\alpha\text{-}PW_9O_{34})_2]^{10-}$, $[(PhSb^{III})_4(A\text{-}\alpha\text{-}GeW_9O_{34})_2]^{12-}$, and $[\{2\text{-}(Me_2NCH_2C_6H_4)Sb^{III}\}_3(B\text{-}\alpha\text{-}As^{III}W_9O_{33})]^{3-}$ were reported. All three compounds are soluble and stable in aqueous solution at physiological pH and they exhibit activity against both *Escherichia coli* and *Bacillus subtilis*.[11] Considering that the organo−Sb(III) species themselves are not water-soluble renders the POM as an inorganic vehicle for the bioactive component, which does not exclude the possibility that the shape and size of the polyanion contribute to this activity, as well. In some follow-up work, we studied the dependence of the POM bioactivity on the type and number of organoantimony groups,[12] and it became apparent that the biological activity of the POM increases with (i) the number of incorporated organoantimony(III) groups and (ii) the type of functional group attached to the antimony atom. Interestingly, the complete absence of any organic moiety completely inactivates the bioactivity of the POM.

To date, only a handful of organoantimony(III)-containing POMs have been synthesized and structurally characterized.[11−13] Here, we report on the synthesis and characterization of three tetra-(*p*-tolyl)antimony(III)-containing POMs and their bioactivity.

EXPERIMENTAL SECTIONExperimental Section

Materials and Physical Measurements

The lacunary POM precursors $Na_9[A\text{-}\alpha\text{-}PW_9O_{34}]\cdot 7H_2O$,[14a] $Na_9[A\text{-}\alpha\text{-}AsW_9O_{34}]\cdot 18H_2O$,[14b] and $Na_9[A\text{-}\alpha\text{-}HGeW_9O_{34}]\cdot 23H_2O$,[14c] and the organoantimony(III) species (*p*-tolyl)$SbCl_2$,[15] were prepared according to the literature. The other reagents were obtained from commercial sources and used as received without further purification. Infrared (IR) spectra were recorded on a Nicolet-Avatar 370 FT-IR spectrometer using KBr pellets in the range of 400–4000 cm^{-1} range. Elemental analyses were performed by Institut des Sciences Analytiques, CNRS, Villeurbanne, France (CHN only), and CREALINS, Villeurbanne, France (all other elements), respectively. Thermogravimetric analyses (TGA) were performed on a TA Instruments SDT Q600 thermobalance at a heating rate of 10 °C min^{-1} under a N_2 atmosphere. The nuclear magnetic resonance (NMR) spectra were recorded on a 400 MHz instrument (JEOL, Modelmodel ECS 400) at room temperature, using 5 mm tubes for ^{1}H, ^{13}C, and ^{31}P NMR, and 10

mm tubes for ^{183}W NMR, with resonance frequencies of 399.78 MHz (^{1}H), 100.71 MHz (^{13}C), 162.14 MHz (^{31}P), and 16.69 MHz (^{183}W)~~, respectively.~~ The chemical shifts are reported with respect to the references Si(CH_3)$_4$ (^{1}H and ^{13}C), 85% H_3PO_4 (^{31}P), and ~~1M~~1 M aqueous Na_2WO_4 (^{183}W)~~, respectively.~~

Synthesis of $Rb_{5.5}Na_{4.5}[\{(p\text{-tolyl})Sb^{III}\}_4(A\text{-}\alpha\text{-}PW_9O_{34})_2]\cdot 40H_2O$ (**RbNa-1-P**)

$Na_9[A\text{-}\alpha\text{-}PW_9O_{34}]\cdot 7H_2O$ (0.050 mmol, 0.128 g) was dissolved in 12 ~~ml~~mL of a 0.5 M NaOAc/AcOH solution (pH 5.6), and then (p-tolyl)$SbCl_2$ (0.050 mmol, 0.0142 g) dissolved in 3 ~~ml~~mL of ethanol was added dropwise under vigorous stirring. The solution ~~color~~ changed from colorless to light yellow. The resulting solution was stirred for 20 min, and then the pH was adjusted from 7.6 to 6.5 by adding 0.5 M HCl_{aq}. The bright solution was stirred for ~~another~~an additional 20 min and filtered, and then a few drops of ~~1M~~1 M $RbCl_{aq}$ were added. This solution was placed in a ~~fridge~~refrigerator at ~~4~~–5 °C. Yellow, rod-shaped crystals of **RbNa-1-P** were obtained after 3 days, which were filtered off and air-dried. Yield: 0.078 g (47 % based on W). Elemental analysis. Calcd (%): ~~Calcd:~~ Sb, 7.37; W, ~~W 50.10~~50.10; P, ~~P 0.94~~0.94; Na, ~~Na~~ 1.57~~,~~; Rb, 7.12~~,~~; C, 5.10~~,~~. Found (%): Sb, 7.21; W, ~~W 48.92~~48.92; P, ~~P 0.93~~0.93; Na, ~~Na~~ 1.89~~,~~; Rb, 7.42~~,~~; C, 5.47. IR (2% KBr pellet, cm~~$^{-1}$~~): 1189 (w), 1072 (s), 1010 (m), 943 (s), 916 (s), 889 (m), 808 (s), 740 (s), 634 (m), 592 (m), 572 (m), 513 (m), 487 (m), 451 (sh), 418 (m).

Synthesis of $(NH_4)_{9.5}Na_{0.5}[\{(p\text{-tolyl})Sb^{III}\}_4(A\text{-}\alpha\text{-}AsW_9O_{34})_2]\cdot 40H_2O$ (**NH_4Na-1-As**)

$Na_9[A\text{-}\alpha\text{-}AsW_9O_{34}]\cdot 18H_2O$ (0.050 mmol, 0.140 g) was dissolved in 12 ~~ml~~mL of water, and then (p-tolyl)$SbCl_2$ (0.050 mmol, 0.0142 g) dissolved in 3 ~~ml~~mL of ethanol was added dropwise under vigorous stirring. The solution ~~color~~ changed from colorless to light yellow. The resulting solution was stirred for 20 min, and then the pH was adjusted from 7.6 to 7.0 by adding 0.5 M HCl_{aq}. The bright solution was stirred for ~~another~~an additional 20 min and filtered, and then a few drops of ~~1M~~1 M NH_4Cl_{aq} were added. This solution was placed in a ~~fridge~~refrigerator at ~~4~~–5 °C. Yellow, needle-shaped crystals of **NH_4Na-1-As** were obtained after 1 week, which were filtered off and air-dried. Yield: 0.086 g (55 % based on W). Elemental analysis. Calcd (%): ~~Calcd:~~ Sb, 7.73; W, ~~W 52.51~~52.51; As, ~~As 2.38~~2.38; Na, ~~Na~~ 0.18~~,~~; N, 2.22~~,~~; C, 5.34~~,~~. Found (%): Sb, 7.83; W, ~~W 51.10~~51.10; As, ~~As 2.44~~2.44; Na, ~~Na~~ 0.21~~,~~; N, 2.31~~,~~; C, 5.83. IR (2% KBr pellet, cm~~$^{-1}$~~): 1156 (w), 1062 (w), 950 (m), 881 (s), 852 (s), 810 (s), 804 (s), 732 (s), 638 (m), 572 (w), 518 (w), 485 (w), 463 (sh), 441 (w), 418 (w).

Synthesis of $Rb_6Na_6[\{(p\text{-tolyl})Sb^{III}\}_4(A\text{-}\alpha\text{-}GeW_9O_{34})_2]\cdot 40H_2O$ (**RbNa-1-Ge**)

$Na_9[A\text{-}\alpha\text{-}HGeW_9O_{34}]\cdot 23H_2O$ (0.050 mmol, 0.145 g) was dissolved in 12 ~~ml~~mL of 0.5 M NaOAc/AcOH buffer (pH 7.0), and then (p-tolyl)$SbCl_2$ (0.050 mmol, 0.0142 g) dissolved in 3 ~~ml~~mL of ethanol was added dropwise under vigorous stirring. The solution ~~color~~ changed from colorless to light yellow. The resulting solution was stirred for 20 min, and then the pH was adjusted from 7.6 to 7.0 by adding 0.5 M HCl_{aq}. The bright yellow solution was stirred for ~~another~~an additional 20 min and filtered, and then a few drops of ~~1M~~1 M $RbCl_{aq}$ were added. This solution was placed in a ~~fridge~~refrigerator at ~~4~~–5 °C. Yellow, rod-shaped crystals of **RbNa-1-Ge** were obtained after 3 days, which were filtered off and air-dried. Yield: 0.092 g (54 % based on W). Elemental analysis. Calcd (%): ~~Calcd:~~ Sb, 7.11; W, ~~W 48.32~~48.32; Ge, ~~Ge 2.12~~2.12; Na, ~~Na~~ 2.35~~,~~; Rb, 7.48~~,~~; C, 5.26~~,~~. Found (%): Sb, 6.67; W, ~~W 47.89~~47.89; Ge, ~~Ge 1.89~~1.89; Na, ~~Na~~ 2.63~~,~~; Rb, 7.51~~,~~; C, 5.83. IR (2% KBr pellet, cm~~$^{-1}$~~): 1189 (w), 1064 (w), 927 (m), 875 (m), 806 (sh), 779 (s), 721 (s), 632 (m), 572 (w), 534 (w), 485 (m), 441 (w).

X-ray Crystallography

The single-crystal X-ray diffraction data of **1-P**, **1-As** , and **1-Ge** were collected on a Bruker Kappa X8 APEX II CCD diffractometer with graphite monochromatic Mo Kα radiation (λ = 0.71073 Å) at 100 K. An empirical absorption correction was applied using the SADABS program.[16] The SHELX software package (Bruker) was used to ~~solve~~determine and refine the structures.[17] The structures were ~~solved~~determined by direct methods and refined by the full-matrix least-squares method ~~([$\sum$~~Σw~~w~~$(|F_0|^2 - |F_c|^2)^2$~~)~~] with anisotropic thermal parameters for all heavy atoms included in the model. The hydrogen atoms of the organic groups were introduced in geometrically calculated positions. The H atoms of the crystal waters were not located. It was not possible to locate all ~~counter cations~~countercations by XRD, due to severe crystallographic disorder, which is a common problem in POM crystallography. Therefore, the exact number of ~~counter cations~~countercations and crystal waters in the compounds was determined by elemental analysis, and the resulting formula units were further used throughout the paper and in the CIF file for overall consistency. In the Supporting Information, the crystal data and ~~structure~~structural refinement for the three compounds are summarized in Table S1 , and selected bond lengths and angles are listed in Tables S2 and S3. Cambridge Crystallographic Data files ~~CCDC~~1965373 ~~1965373~~ (**NaRb-1-P**), ~~CCDC~~1965371 ~~1965371~~ (**NH_4-1-As**), and ~~CCDC~~1965372 ~~1965372~~ (**NaRb-1-Ge**) contain the supplementary crystallographic data for this paper. These data can be obtained free of charge from the Cambridge Crystallographic Data Center via www.ccdc.cam.ac.uk/ .

Antibacterial Activity: Determination of Minimal Inhibitory Concentrations (~~MIC~~MICs) for Bacterial Cells

The MIC studies were conducted in MHB media and followed our earlier work.[11] The Gram-positive bacteria ~~*Bacillus*~~*B. subtilis* ~~,~~ as well as the Gram-negative bacteria ~~*Escherichia*~~*E. coli* K12, ~~*Vibrio parahaemolyticus*~~*V. parahemolyticus*, and *V. vulnificus* were used in the assay. *Vibrio* species are well -known pathogens to not only humans~~,~~ but also economically important aquaculture stocks. In 2016, Vezzulli et al. described an increasing abundance of pathogenic *Vibrio* species in temperate and cold regions, such as the North Sea, with warming sea surface water temperatures.[18] Two North Sea isolates of *V.* ~~*parahaemolyticus*~~*parahemolyticus and V. vulnificus* were chosen to represent their closely related human~~-~~pathogenic strains in the MIC. The starting concentration of polyanions **1-P**, **1-As**, and **1-Ge** and the phenylantimony(III)~~-~~analogues $Rb_9Na[(PhSb^{III})_4(A\text{-}\alpha\text{-}PW_9O_{34})_2]\cdot 20H_2O$ (**RbNa-2-P**),[11] $Cs_{6.5}Na_{3.5}[(PhSb^{III})_4(A\text{-}\alpha\text{-}AsW_9O_{34})_2]\cdot 36H_2O$ (**CsNa-2-As**),[12c] and $(NH_4)_{12}[(PhSb^{III})_4(A\text{-}\alpha\text{-}GeW_9O_{34})_2]\cdot 20H_2O$ (**NH 4 -2-Ge**),[11] in deionized water used in the MIC assay plates was 10 mg ~~ml~~mL~~-~~$^{-1}$. The MIC was ~~conducted~~determined in triplicate for each strain and polyanion.

Antitumor Activity: Cytotoxicity Tests in Human Cancer Cells

Cells and ~~culture conditions~~Culture Conditions. Three different human cancer cell lines, A549 (non-small cell lung cancer), CH1/PA-1 (ovarian teratocarcinoma), and SW480 (colon carcinoma), were used ~~for cytotoxicity determination~~to determine cytotoxicity. A549 and SW480 cells were kindly provided by ~~Brigitte~~B. Marian~~,~~ (Institute of Cancer Research, Department of Medicine I, Medical University Vienna, Vienna, Austria). CH1/PA-1 cells were provided by ~~Lloyd~~L. R. Kelland~~,~~ (CRC Center for Cancer Therapeutics, Institute of Cancer Research, Sutton, U.K.). All cell culture media, supplements, and reagents were purchased from Sigma-Aldrich, unless stated otherwise. Cells were grown as adherent monolayer cultures in minimal essential medium (MEM) supplemented with 10% heat-inactivated fetal bovine serum (FBS; from BioWest), 4 mM ~~L~~-L -glutamine, 1 mM sodium pyruvate, and 1% (v/v ~~nonessential~~) non-essential amino acids (from ~~100x~~a 100× solution). The cultures were kept at 37 °C in a humidified incubator in an atmosphere containing 5% CO_2 in air. Human ~~Foreskin Fibroblasts~~foreskin fibroblasts (HFF-1) (ATCC® SCRC-1041) at a low~~-~~passage~~-~~number (~~less than~~ <30) were grown as monolayers in ~~Dulbecco's Modified Eagle's Medium~~Dulbecco's modified Eagle's medium (DMEM) (Sigma-Aldrich, ~~Saint~~St. Louis, MO~~, U.S.A.)~~ supplemented with 15% heat -inactivated FBS (Sigma-Aldrich) and a 1% antibiotic solution (~~Penicillin~~penicillin ~~Streptomycin™~~streptomycin, Sigma-Aldrich).

Cell Viability Assay. The IC_{50} (50% inhibitory concentration) values of the tested polyanions on tumor cells were determined by means of the colorimetric MTT (thiazolyl blue tetrazolium bromide) staining method. Three different cell densities were plated into 96-well plates (Starlab International GmbH, Hamburg, Germany), depending on the cell line: 3~~-x~~× 10^3 A549 cells/well, 1~~-x~~× 10^3 CH1/PA-1 cells/well, and 2~~-x~~× 10^3 SW480 cells/well, each in volumes of 100 µL/well. After a 24 h ~~pre-incubation~~preincubation, cells were treated in ~~triplicates~~triplicate with a range of concentrations of the polyanions dissolved directly in MEM. After a 96 h incubation at 37 °C, the medium from each well was replaced with 100 µL of 6:1 ~~RPMI~~rpmI 1640 medium (supplemented with 10% heat-inactivated FBS and 1 mM sodium pyruvate~~):~~ /MTT solution ~~(~~[250 mg of MTT in 50 mL of Dulbecco's phosphate -buffered saline (PBS~~))~~]. The plates were incubated for a further 4 h, and the resultant formazan crystals were dissolved in 150 µL of DMSO. ~~Absorbance~~The absorbance was determined spectrophotometrically at 550 nm with a microplate reader (ELx880, BioTek) using a reference wavelength of 690 nm. All tests comprised at least three independent experiments. The cell viability was measured in HFF-1 cells using the MTS [3-(4,5-dimethylthiazol-2-yl)-5-(3-~~carboxymethoxyphenyl~~carboxymethoxyphenyl)-2-(4-sulfophenyl)-~~2H~~2*H* -tetrazolium] assay, as described by Cavalli et al. ~~in 2012.~~[19] HFF-1 cells were seeded in 96-well plates at ~~a density~~densities of 7~~-x~~× 10^3, 6~~-x~~× 10^3 , and 5~~-x10~~× 10^3 cells/well and incubated with serial concentrations of the polyanions, ranging from 100 ~~µM~~ to 0.015 µM, for 24, 48, and 72 ~~hoursh~~, respectively. Cell viability was determined by the CellTiter 96® Proliferation Assay Kit (Promega, Madison, W~~I, USA~~) according to the manufacturer's instructions, and absorbances were measured by Multiskan™ FC ~~Microplate~~microplate photometer (ThermoScientific~~, USA~~) at 490 nm. The effect on cell viability at different concentrations was expressed as a percentage, by comparing absorbances of treated cells with those of cells incubated with culture medium alone. The IC_{50} and 95% confidence intervals (CIs) were determined using Prism software (Graph-Pad Software, San Diego, CA~~, USA~~).

Apoptosis ~~assay~~Assay. Induction of programmed cell death by the compounds was ~~determined~~assessed by the flow-cytometric annexin V/PI assay. SW480 cells were seeded ~~into~~in 24-well plates (Starlab) at a density of ~~7x10~~7 × 10^4 cells in 600 µL of complete MEM per well. After a 24 h ~~pre-incubation~~preincubation, cells were treated with different concentrations (0.016 ~~µM~~, 0.08 ~~µM~~, 0.4 ~~µM~~, and 2 µM) of the tested polyanions, dissolved directly in the medium.

Only for polyanion **2-Ge** were higher concentrations (50 μM, 10 μM, 2 μM, and 0.4 μM) were used, due to the higher IC_{50} values. After exposure for 24 h at 37 °C, the supernatant of each well was collected, and the cells were trypsinized and mixed with the supernatant. The cells were pelleted by centrifugation (300 *g*, for 3 min), and the supernatant was removed. Then, the cells were resuspended with FITC-conjugated annexin V (0.4 μg/mL) (BioVision) in binding buffer ([10 mM HEPES/NaOH (pH 7.4), 140 mM NaCl, and 2.5 mM $CaCl_2$)] and incubated at 37 °C for 15 min. The staining with propidium iodide (1.6 μg/mL) (PI, Fluka) was doneperformed shortly before the measurement with a Millipore guava easyCyte 8 HT flow cytometer and InCyte software. The received dot plots were analyzed with the FlowJo software (TreeStar).

RESULTS AND DISCUSSIONResults and Discussion

Structural Characterization

The polyanion $[\{(p\text{-tolyl})Sb^{III}\}_4(A\text{-}\alpha\text{-}AsW_9O_{34})_2]^{10-}$ (**1-As**) was prepared by reaction of (*p*-tolyl)$SbCl_2$ with the POM precursor salt $Na_9[A\text{-}\alpha\text{-}AsW_9O_{34}]\cdot 18H_2O$ in water. The (*p*-tolyl)$SbCl_2$ was first dissolved in 3 mlmL of ethanol and then added dropwise to an aqueous solution of the lacunary POM precursor. The product was isolated as the mixed ammonium–sodium salt $(NH_4)_{9.5}Na_{0.5}[\{(p\text{-tolyl})Sb^{III}\}_4(A\text{-}\alpha\text{-}AsW_9O_{34})_2]\cdot 40H_2O$ (**NH 4 Na-1-As**). The isostructural polyanions $[\{(p\text{-tolyl})Sb^{III}\}_4(A\text{-}\alpha\text{-}PW_9O_{34})_2]^{10-}$ (**1-P**) and $[\{(p\text{-tolyl})Sb^{III}\}_4(A\text{-}\alpha\text{-}GeW_9O_{34})_2]^{12-}$ (**1-Ge**) were synthesized equally by reaction of (*p*-tolyl)$SbCl_2$ with the relevant sodium salts of the lacunary POM precursors $Na_9[A\text{-}\alpha\text{-}PW_9O_{34}]\cdot 7H_2O$ and $Na_9[A\text{-}\alpha\text{-}HGeW_9O_{34}]\cdot 23H_2O$ in 0.5 M NaOAc/AcOH solutions at pH 6.5 and 7, respectively. The polyanions were then crystallized as mixed rubidium–sodium salts, resulting in $Rb_{5.5}Na_{4.5}[\{(p\text{-tolyl})Sb^{III}\}_4(A\text{-}\alpha\text{-}PW_9O_{34})_2]\cdot 40H_2O$ (**RbNa-1-P**) and $Rb_6Na_6[\{(p\text{-tolyl})Sb^{III}\}_4(A\text{-}\alpha\text{-}GeW_9O_{34})_2]\cdot 40H_2O$ (**RbNa-1-Ge**), respectively. The X-ray structural analysis revealed that **1-P**, **1-As** , and **1-Ge** are isostructural and they crystallize in the triclinic crystal system, in space group $P\bar{1}$. The three polyanions comprise four (*p*-tolyl)Sb^{III} groups sandwiched by two $\{A\text{-}\alpha\text{-}XW_9O_{34}\}$ (X = P, As, or Ge) Keggin fragments, resulting in a structure with idealized C_{2h} symmetry (see Fig.Figure 1). Each Sb^{III} atom is tetra coordinatedtetracoordinated by two oxygens of one Keggin unit, one oxygen of the other Keggin unit, and a C atom of the terminal tolyl group. This results in a see sawseesaw geometry with the bulky *p*-tolyl groups pointing outside the polyanion, leaving space on the inside for the lone pair of electrons. The bond lengths of Sb–O ([2.014(7)–2.411(11) Å)] and Sb–C ([2.112(10)–2.192(7) Å)] bond lengths are within the usual ranges. Bond valence sum (BVS) calculations confirm that the oxidation state of all antimony atoms is +3.[20] The Sb···Sbdistances for the three polyanions are 3.56 Å for **1-As** and **1-P** and 3.57 Å for **1-Ge** (see Figure 1). The phenyl derivatives of **1-As**, **1-P** , and **1-Ge** are also known, $[(PhSb^{III})_4(A\text{-}\alpha\text{-}XW_9O_{34})_2]^{n-}$ ([X = P (**2-P**), As (**2-As**), or Ge (**2-Ge**))]. [11,12c]

Figure 1. (a) Combined polyhedral/ball-and-stick representation of $[\{(p\text{-tolyl})Sb^{III}\}_4(A\text{-}\alpha\text{-}XW_9O_{34})_2]^{n-}$ ([X = P (**1-P**), As (**1-As**), or Ge (**1-Ge**))]. (b) Top view of the positions of the four antimony atoms describing a rectangle. Color code: WO_6, red octahedra; heteroatom X, purple; Sb, green; C, gray; H, black balls.

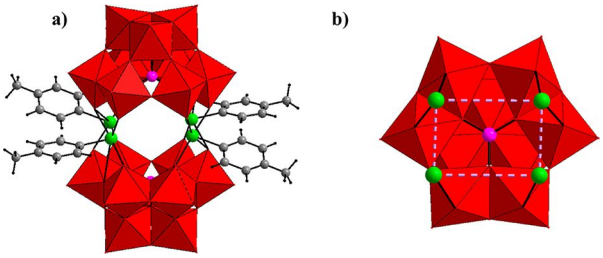

Equations for the synthesis of **1-P**, **1-As** , and **1-Ge** are shown below, and they indicate that the ideal molar ratio of the reagents (*p*-tolyl)$SbCl_2$ and trilacunary POM precursor should be 2:1.

4
(*p*-tolyl)SbCl2+2
→+8
Cl−

4

(*p*-tolyl)SbCl2 + 2 → + 8 Cl−

4 (*p*-tolyl)SbCl2 + 2 → + 8 Cl−

The yield following such a stoichiometry was only around 10%. However, when using an equimolar ratio, the yield increased to 47–55%. Numerous control experiments revealed that the key factors affecting the yields for polyanions **1-As**, **1-P** , and **1-Ge** are solvent (water vs sodium acetate buffer) and pH.

Infrared (IR) spectroscopy

Fourier-transform infrared (FT-IR) spectra were recorded of **RbNa-1-P**, **NH 4 Na-1-As**, and **RbNa-1-Ge** were recorded (see Supporting Information, Figures S1–3–S3). The stretching and bending vibrations of the C–H and C–C bonds of the *p*-tolyl groups appear at 1189, 1072, and 740 cm−1 for **1-P**, in the range of 1156, 1062, and 732 cm−1 for **1-As**, and 1189, 1064, and 721 cm−1 for **1-Ge**. For **1-P**, the band at 1072 cm−1 corresponds to the P–O stretching mode. The band at 852 cm−1 corresponds to the As–O stretching mode for **1-As**, whereas the band at 875 cm−1 corresponds to the Ge–O stretching mode for **1-Ge**. The peaks below 1000 cm−1 are attributed to the terminal W=O bonds as well as the bridging W–O–W stretching modes for all three polyanions.

Thermogravimetric analysis

We investigated the thermal stability of **RbNa-1-P**, **NH 4 Na-1-As**, and **RbNa-1-Ge** by thermogravimetric analysis (TGA), (see the Supporting Information, Figure S4). The experiments were performed in the temperature range 20 — of 20–800 °C range under a N_2 atmosphere. Several weight-loss steps were observed for all three compounds. The first step in the range of 20–140 °C is associated with the loss of crystal waters. The number of crystal waters determined by TGA was slightly lower than that found by elemental analysis. The reason could be the drying of the samples at room temperature prior to the measurements. For **1-As** , the second weight-loss step in the range of 140 – 400 °C can be assigned to the loss of all 4four tolyl groups and 6six NH_3 molecules per formula unit (7.5% found vs 7.5% calculated). Some of the other NH_3 molecules are possibly lost already below 140 °C. For **1-P** and **1-Ge**, it was difficult to determine the exact weight loss steps for the organic groups. The total weight losslosses for **1-As**, **1-P** , and **1-Ge** at 800 °C waswere 20.4%, 15.8%, and 17.6%, respectively.

Multinuclear NMR Spectroscopy

The solution stability of polyanions **1-P**, **1-As** , and **1-Ge** was investigated by multinuclear NMR spectroscopy after redissolution of the solid salts in water. The ^{183}W NMR spectra of **1-P** (–101.7,–113.1,–115.6,–168.2, and −177.4 ppm) and **1-As** (–83.0,–90.0,–109.4,–144.8,–and −173.3 ppm) showed the expected five peaks with intensity ratios of 2:1:2:2:2 and 2:2:1:2:2, respectively, which is fully consistent with the C_{2h} point group symmetry of the polyanions in the solid state (see Figure 2). No ^{183}W NMR spectrum could be obtained for **1-Ge** due to the low solubility of this compound.

Figure 2. ^{183}W NMR spectra of **1-P** (left) and **1-As** (right) recorded in H_2O/D_2O at room temperature.

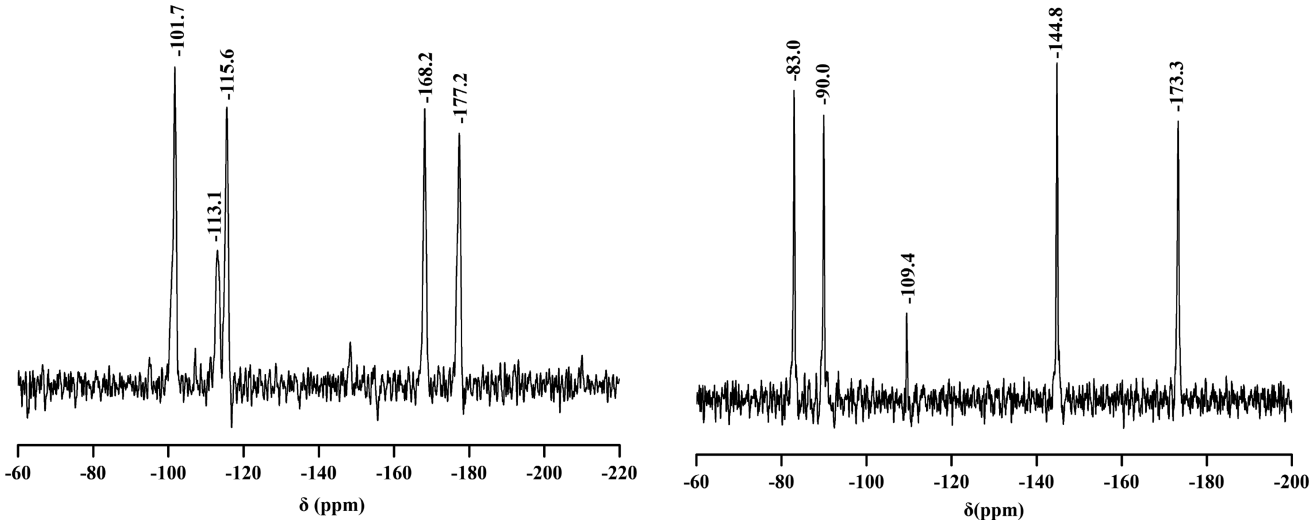

The ^{31}P NMR spectrum of **1-P** displayed the expected singlet at ~~–~~11.2 ppm (see Figure 3). The ^{13}C NMR spectra of **1-P**, **1-As** , and **1-Ge** were as expected, indicating the coordinated *p*-tolyl groups (Figure S5). The ^{1}H NMR spectra of **1-P**, **1-As** , and **1-Ge** also showed the presence of the *p*-tolyl groups (Figure S6). Additionally, time-dependent ^{1}H NMR spectra were recorded for all three compounds, and demonstrated their stability in aqueous solution for at least 5 days (Figure S7). The reagent (*p*-tolyl)$SbCl_2$ is not soluble in aqueous solution, and hence, no NMR studies could be performed in this solvent.

Figure 3. ^{31}P NMR spectrum of **1-P** recorded in H_2O/D_2O at room temperature.

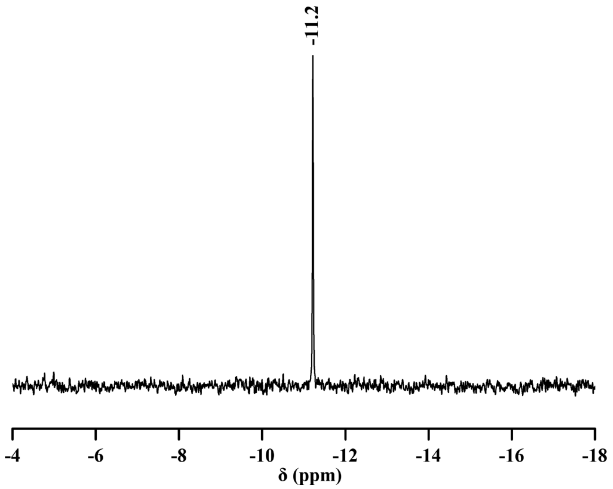

Antibacterial Activity: Determination of Minimal Inhibitory Concentrations (~~MIC~~MICs) for Bacterial Cells

The antibacterial ~~activity~~activities of the three lacunary POM precursors [*A*-α-$PW_9O_{34}]^{9-}$, [*A*-α-$AsW_9O_{34}]^{9-}$, and [*A*-α-$HGeW_9O_{34}]^{9-}$ and their {(*p*-tolyl)Sb}~~–~~derivatives **1-P**, **1-As** , and **1-Ge** against four different kinds of bacteria (*E. coli*, *B. subtilis*, *V. ~~parahaemolyticus~~parahemolyticus* , and *V. vulnificus*) are listed in Table 1 . All three POM precursors showed no inhibition against bacterial growth. In contrast, the {(*p*-tolyl)Sb^{III}}-substituted polyanions **1-P**, **1-As** , and **1-Ge** successfully inhibited the selected bacterial strains. The ~~bioactivity~~bioactivities of these ~~was~~were compared with that of our earlier reported isostructural ~~tetra~~tetraphenylantimony ~~phenylantimony~~ containing polyanions **2-P**, **2-As** , and **2-Ge**, respectively (see Table S4). [11,12c] Our results demonstrate that the three novel polyanions **1-P**,

1-As , and **1-Ge** exhibit ~~a similar~~ inhibitory ~~activity~~activities against the four bacterial strains ~~as~~similar to those of the phenyl-Sb-containing analogues **2-P**, **2-As** , and **2-Ge**. While the former showed a ~~minimum inhibitory concentration (MIC)~~ in the range of 15.6 ~~–~~ 62.5 μg/~~ml~~mL, the MICs for the latter ranged from 15.6 ~~–~~to 110 μg/~~ml~~mL (see Table S4). Thus, the relationship between the type of organic group (*p*-tolyl vs phenyl) attached to the polyanions and their apparent biological activity is supported by these findings. We show the MIC results of all organo-Sb^{III}-containing heteropolytungstates against the growth of *E. coli* and *B. subtilis* in Table 2 , which is arranged by increasing antibacterial activity. The three novel (*p*-tolyl)Sb^{III}-containing **1-P**, **1-As** , and **1-Ge** exhibit the strongest bioactivity of all known organoantimony-containing POMs.

~~To date, we have explored organoantimony POMs with three different types of organic groups attached to Sb^{III}, such as phenyl, (*ortho*-Me_2NCH_2)phenyl (Hyp), and *para*-tolyl. We have shown in earlier work that the phenyl-Sb POMs display significantly higher antibacterial activity than their isostructural Hyp-Sb analogues.[12b] Hence it appears that *ortho*-functionalization of the phenyl ring is not promising. Furthermore, bioactivity increases with the number of the organic groups attached to the polyanion.[12a] On the other hand, in the absence of any organo-group on Sb^{III}, the bioactivity of the resulting polyanion is very poor.[12c] Our current work demonstrates that *para*-functionalization of the phenyl ring results in even slightly better bioactivity than for the phenyl-Sb POMs. As the *para*-position on the phenyl ring protrudes away from the polyanion and is well exposed to the biotarget it appears likely that even larger *para*-substituents such as ethyl or iso-propyl might be even more effective.~~

Table 1. Minimal ~~inhibitory concentration~~Inhibitory Concentrations (~~MIC~~MICs) for ~~different polyanions~~Different Polyanions against the ~~growth~~Growth of ~~bacteria.~~Bacteria

	MIC ~~determination~~[K] (μg/mL)[T] ~~(μg/ ml)~~			
	1-P	**1-As**	**1-Ge**	$[XW_9O_{34}]^{n-}$
Gram-positive				
~~*Bacillus*~~*B. subtilis*	15.6	15.6	15.6	~~–~~[a]
Gram-negative				
~~*Escherichia*~~*E. coli*	62.5	31.2	15.6	~~–~~
~~*Vibrio parahaemolyticus*~~*V. parahemolyticus*	15.6	31.2	15.6	~~–~~
V. vulnificus	15.6	15.6	15.6	~~–~~

[a]No bacterial inhibition was found for the three lacunary POM precursors.

Table 2. Minimal ~~inhibitory concentration~~Inhibitory Concentrations (~~MIC~~MICs) of ~~various organoantimony~~Various Organoantimony ~~containing heteropolytungstates~~Containing Heteropolytungstates against the ~~growth~~Growth of ~~*Escherichia*~~*E. coli* and ~~*Bacillus*~~*B. subtilis* .

	MIC ~~determination~~[K] (μg/mL)[T] ~~(μg/ ml)~~		
~~Organoantimony~~organoantimony(III)-containing POMs	*B. subtilis*	*E. coli*	~~Ref~~ref
$[Na\{2\text{-}(Me_2HN^+CH_2)C_6H_4S\text{-}b^{III}\}As^{III}_2W_{19}O_{67}(H_2O)]^{10-}$ ~~–~~ [K]**(1-Hyp)**[T] ~~(1-Hyp)~~	250	1000	12b
$[(Sb^{III}OH)_4(A\text{-}\alpha\text{-}As^VW_9O_{34})_2]^{10-}$ ~~–~~ [K]**(1-SbOH)**[T] ~~(1-SbOH)~~	250	1000	12c

Organoantimony(III)-containing POMs	MIC determination (μg/mL) *B. subtilis*	*E. coli*	Ref
[{2-($Me_2HN^+CH_2$)$C_6H_4Sb^{III}$}$_2As^{III}_2W_{19}O_{67}(H_2O)]^{8-}$ (**2-Hyp**)	250	500	12b
[($PhSb^{III}$){$Na(H_2O)$}$As^{III}_2W_{19}O_{67}(H_2O)]^{11-}$ (**1-PhSb**)	125	500	12a
[($PhSb^{III}$)$_2As^{III}_2W_{19}O_{67}(H_2O)]^{10-}$ (**2-PhSb**)	62.5	250	12a
[{2-($Me_2HN^+CH_2$)$C_6H_4Sb^{III}$}$_3$(*B*-α-$As^{III}W_9O_{33}$)]$^{3-}$ (**3-Hyp**)	60	130	11
[($PhSb^{III}$)$_3$(*B*-α-$As^{III}W_9O_{33}$)$_2$]$^{12-}$ (**3-PhSb**)	62.5	125	12a
[($PhSb^{III}$)$_4$(*A*-α-PW_9O_{34})$_2$]$^{10-}$ (**2-P**)	50	110	11
[($PhSb^{III}$)$_4$(*A*-α-GeW_9O_{34})$_2$]$^{12-}$ (**2-Ge**)	80	80	11
[($PhSb^{III}$)$_4$(*A*-α-$As^VW_9O_{34}$)$_2$]$^{10-}$ (**2-As**)	15.6	62.5	12c
[{(*p*-tolyl)Sb^{III}}$_4$(*A*-α-PW_9O_{34})$_2$]$^{10-}$ (**1-P**)	15.6	62.5	This work
[{(*p*-tolyl)Sb^{III}}$_4$(*A*-α-$As^VW_9O_{34}$)$_2$]$^{10-}$ (**1-As**)	15.6	31.3	This work
[{(*p*-tolyl)Sb^{III}}$_4$(*A*-α-GeW_9O_{34})$_2$]$^{11-}$ (**1-Ge**)	15.6	15.6	This work

To date, we have explored organoantimony-containing POMs with three different types of organic groups attached to Sb^{III}, such as phenyl, (*o*-Me_2NCH_2)phenyl (Hyp), and *p*-tolyl. We have shown in earlier work that the phenyl-Sb POMs display antibacterial activity significantly higher than those of their isostructural Hyp-Sb analogues.[12b] Hence it appears that *ortho* functionalization of the phenyl ring is not promising. Furthermore, bioactivity increases with the number of organic groups attached to the polyanion.[12a] On the other hand, in the absence of any organo group on Sb^{III}, the bioactivity of the resulting polyanion is very poor.[12c] Our current work demonstrates that *para* functionalization of the phenyl ring results in even slightly better bioactivity than for the phenyl-Sb POMs. As the *para* position on the phenyl ring protrudes away from the polyanion and is well exposed to the biotarget, it appears likely that even larger *para* substituents such as ethyl or isopropyl might be even more effective.

Cytotoxicity in Cancer Cells

The cytotoxic potency of **1-P**, **1-As** , and **1-Ge** in human tumor cell lines was investigated. The first POM-based example of that type was reported in 1965 by Mukherjee, using a mixture of $H_3[PW_{12}O_{40}]$ and caffeine for the treat-

ment of gastrointestinal cancer.[21] The high toxicity of purely inorganic POMs restricts their clinical application. Organic–inorganic hybrid POMs are conceived as potential anticancer reagents.[6f] Here we investigated the cytotoxic effects of six organoantimony-containing POMs, the novel **1-P**, **1-As**, and **1-Ge** and the phenyl-analogues **2-P**, **2-As**, and **2-Ge**, against A549 (non-small cell lung cancer), CH1/PA-1 (ovarian teratocarcinoma), and SW480 (colon carcinoma) cells by using an MTT assay.

In general, the cytotoxic potency of the novel *p*-tolylantimony(III)-containing polyanions **1-P**, **1-As**, and **1-Ge** is higher in the broadly chemosensitive ovarian carcinoma (CH1/PA-1) and in colon carcinoma (SW480) cells (with promising IC_{50} values mostly in the two-digit nanomolar range) than in the more chemoresistant non-small lung cancer (A549) cell line (Table 3). All three **1-P**, **1-As** , and **1-Ge** all showed similar cytotoxicity, which was higher in all of the investigated cell lines than that of the three phenylantimony(III)-containing analogues **2-P**, **2-As** , and **2-Ge** (with **2-Ge** showing the lowest potency by far), (see Figure 4). Interestingly, all six investigated polyanions exerted a significantly loweran antiproliferative activity in human foreskin fibroblasts that was significantly lower than the activity observed in cancer cells, indicating a specific antitumor activity (Table 4). Only **2-Ge** exhibited a higher IC_{50} value in one cell line (A549) than the value obtained in HFF-1. As reported in Table 4 , the three *p*-tolyl-POMs **1-P**, **1-As** , and **1-Ge** exerted a variable effecteffects on the viability of human foreskin fibroblasts generating dose–response curves. Among them, polyanion **1-Ge** was the least toxic, showing the highest IC_{50} values, ranging from 3.16 µM to 1.92 µM over time, exerting a minor cell alteration; polyanion **1-As** exhibited the lowest value of IC_{50} (<1 µM) at all of the time–points analyzed. The cells treated with **1-P**, **1-As** , and **1-Ge** displayed an increasing phenotypical cell alteration microscopically over time. The dose–response curves for the phenyl–derivatives **2-P**, **2-As** , and **2-Ge** indicated that **2-Ge** affected the cell viability the least at the 24-hour-intervalh time point, exhibiting a significantly higheran IC_{50} value (2.05 µM) significantly higher than those of both **2-P** and **2-As** with IC_{50} values of 1.37 µM and 1.35 µM, respectively. At 72-hourshour post-treatment, all three phenyl–derivatives exhibited similar effects on cell viability, with IC_{50} values of 3.55 µM, 3.98 µM, and 3.54 µM for **2-P**, **2-Ge** , and **2-As**, respectively. Overall, the performed experiments suggest that for organoantimony-containing POMs, the presence of the phenyl group is associated with a minor effect on cell viability compared with the corresponding *p*-tolyl group, with the exception of **2-Ge** at 24-hourshour. Indeed, the phenyl–derivative **2-As** exhibited significantly less cytotoxicity than the corresponding *p*-tolyl–derivative **1-As** at all of the time–points investigated ($p < 0.0001$).

Table 3. IC_{50} valuesValues of the investigated polyanionsInvestigated Polyanions for three different cancer cell linesThree Different Cancer Cell Lines after Incubation for 96 hours incubation.h

Compound compound	IC_{50} [(µM)][a]		
	A549	CH1/PA-1	SW480
1-P	0.20[K]0.20 ± 0.02[T] ± 0.02	0.0097[K]0.0097 ± 0.0006[T] ± 0.0006	0.0093[K]0.0093 ± 0.0032[T] ± 0.0032
1-As	0.21[K]0.21 ± 0.02[T] ± 0.02	0.010[K]0.010 ± 0.002[T] ± 0.002	0.010[K]0.010 ± 0.003[T] ± 0.003
1-Ge	0.28[K]0.28 ± 0.03[T] ± 0.03	0.010[K]0.010 ± 0.002[T] ± 0.002	0.016[K]0.016 ± 0.004[T] ± 0.004
2-P	0.62[K]0.62 ± 0.09[T] ± 0.09	0.037[K]0.037 ± 0.005[T] ± 0.005	0.025[K]0.025 ± 0.005[T] ± 0.005
2-As	0.53[K]0.53 ± 0.02[T] ± 0.02	0.031[K]0.031 ± 0.002[T] ± 0.002	0.019[K]0.019 ± 0.002[T] ± 0.002
2-Ge	17[K]17 ± 2[T] ± 2	0.29[K]0.29 ± 0.02[T] ± 0.02	0.82[K]0.82 ± 0.22[T] ± 0.22

[a]Mean 50 % inhibitory concentration ± the standard deviationsdeviation in A549, CH1/PA-1, and SW480 cell lines, determined by the MTT assay.

Figure 4. Concentration–effect curves of polyanions **1-P**, **1-As**, **1-Ge**, **2-P**, **2-As**, and **2-Ge** in A549, CH1/PA-1, and SW480 cells, determined by the MTT assay (96 h exposure). The dashed lines denote the 50% inhibitory level.

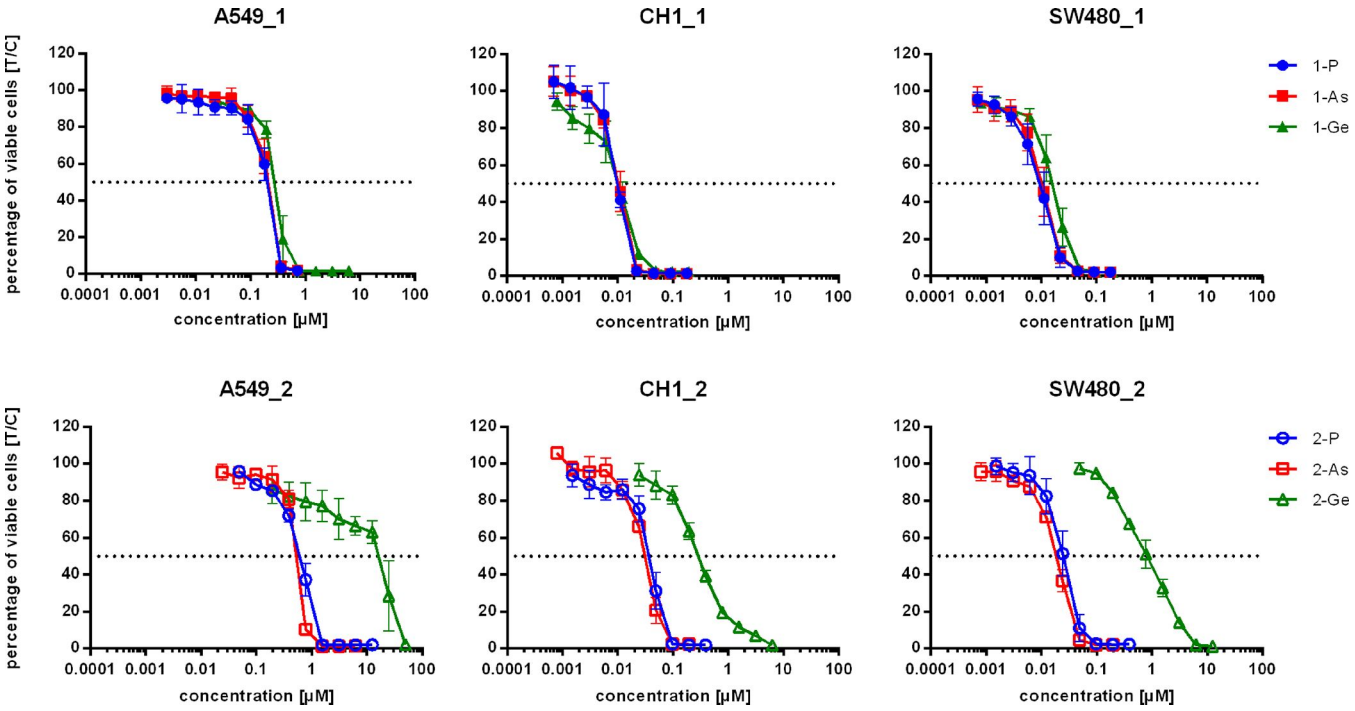

Table 4. ~~Inhibitory concentration 50 (IC_{50}, µM)~~Values and 95% ~~confidence interval values~~Confidence Interval Values for **1-P**, **1-As**, and **1-Ge** and ~~the phenyl derivatives~~Phenyl Derivatives **2-P**, **2-As**, and **2-Ge** ~~at~~ 24, 48, and 72 ~~hours post-treatment~~h after Treatment in HFF-1 ~~cells.~~Cells

~~Compound~~ compound	IC_{50} ~~[~~(µM~~]~~)[a]		
	24 ~~hpth~~	48 ~~hpth~~	72 ~~hpth~~
1-P	1.44 (K(1.27–1.62)T ~~1.27 - 1.62)~~	1.12 (K(0.79–1.59)T ~~0.79 - 1.59)~~	1.34 (K(1.08–1.66)T ~~1.08 - 1.66)~~
1-As	0.53 (K(0.46–0.59)T ~~0.46 0.59)~~	0.58 (K(0.43–0.77)T ~~0.43 - 0.77)~~	0.82 (K(0.66–1.01)T ~~0.66 - 1.01)~~
1-Ge	3.16 (K(2.84–3.52)T ~~2.84 - 3.52)~~	2.03 (K(1.23–3.31)T ~~1.23 - 3.31)~~	1.92 (K(1.75–2.10)T ~~1.75 - 2.10)~~
2-P	1.37 (K(1.28–1.45)T ~~1.28 - 1.45)~~	2.38 (K(0.06–5.17)T ~~0.06 - 5.17)~~	3.55 (K(2.92–4.32)T ~~2.92 - 4.32)~~
2-As	1.35 (K(1.26–1.44)T ~~1.26 - 1.44)~~	3.33 (K(2.59–4.27)T ~~2.59 - 4.27)~~	3.54 (K(2.80–4.47)T ~~2.80 - 4.47)~~
2-Ge	2.05 (K(1.83–2.28)T ~~1.83 - 2.28)~~	3.72 (K(3.12–4.43)T ~~3.12 - 4.43)~~	3.98 (K(3.27–4.84)T ~~3.27 - 4.84)~~

[a]Mean 50 % inhibitory concentration and 95% confidence ~~intervals~~interval (~~CIs~~CI) in the HFF-1 cell line, determined by the MTS assay.

Apoptosis ~~assay~~Assay

SW480 cells were exposed to the polyanions to determine the extent of apoptosis ~~induction~~induced by annexin V-FITC/PI ~~–~~staining and flow cytometry. Polyanions **1-P**, **1-As**, **1-Ge**, **2-P** , and **2-As** at a concentration of 2 µM induced apoptosis in a very high percentage of cells, ranging from 84% to 93% after a 24 h exposure (Table S6 and

Figure 5). At a concentration of 0.4 µM, the highest level of induced apoptosis induction (46% and 49%) was detected for two of the phenylantimony(III)-containing heteropolytungstates (**2-P** and **2-As**). In the case of the three *p*-tolylantimony(III)-containing heteropolytungstates (**1-P**, **1-As** , and **1-Ge**), apoptosis was pronounced, with percentages ranging between from 22% and to 30% (Figure S8). **2-Ge** showed the lowest capacity of apoptosis induction, which correlates very well with the measured IC_{50} values.

Figure 5. SW480 cells were labelled labeled with annexin V-FITC and PI to analyze apoptosis the induction of apoptosis by **1-P**, **1-As**, **1-Ge**, **2-P**, **2-As**, and **2-Ge** after 24 h. Depicted are dot plots from flow cytometric analysis of samples exposed to the highest concentration of the studied compounds ([2 µM, except for **2-Ge** : (50 µM)]. The upper top left quadrants represent necrotic (Q1 :, AV–/PI+), the upper top right quadrants late apoptotic (Q2 :, AV+/PI+), the lower bottom right quadrants early apoptotic (Q3 :, AV+/PI – –), and the lower bottom left quadrants viable (Q4 :, AV–/PI – –) cell fractions. One representative experiment out of three is shown.

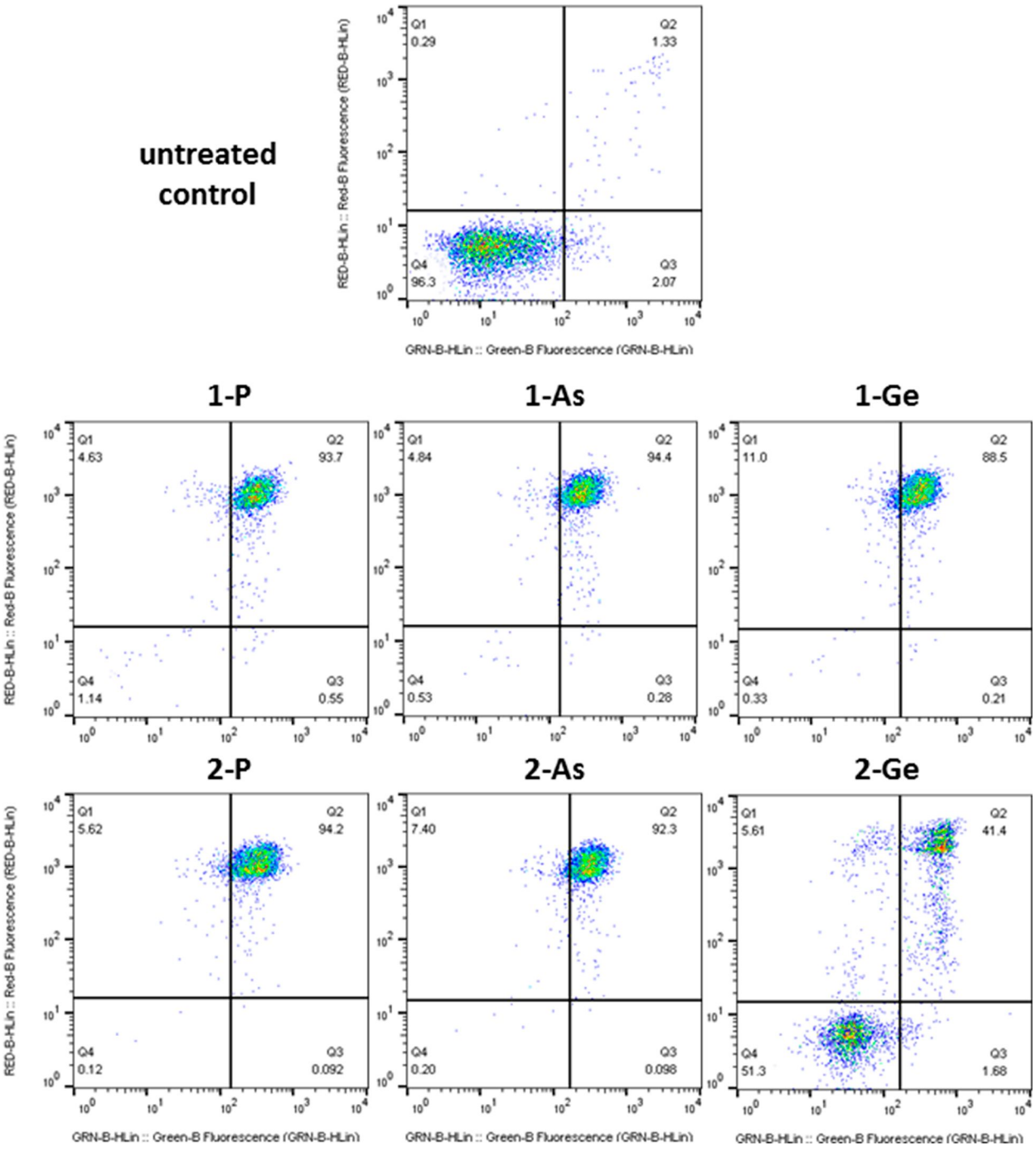

~~CONCLUSIONS~~Conclusions

We have prepared the three dimeric, sandwich-type tetra-(*p*-tolyl)Sb-containing heteropoly-18-tungstates [{(*p*-tolyl)Sb^{III}}$_4$(*A*-α-PW_9O_{34})$_2$]$^{10-}$ (**1-P**), [{(*p*-tolyl)Sb^{III}}$_4$(*A*-α-AsW_9O_{34})$_2$]$^{10-}$ (**1-As**), and [{(*p*-tolyl)Sb^{III}}$_4$(*A*-α-$Ge^{IV}W_9O_{34}$)$_2$]$^{12-}$ (**1-Ge**), which were characterized by single-crystal XRD, FT-IR, and multinuclear (^{1}H, ^{13}C, ^{31}P,

and ^{183}W) NMR in solution. The novel **1-P**, **1-As**, and **1-Ge** and their phenyl–analogues **2-P**, **2-As**, and **2-Ge** have been explored for antibacterial and *in vitro* anticancer activity. This is the first study to test the antimicrobial effect of these compounds against the human pathogens *V. parahaemolyticusparahemolyticus* and *V. vulnificus*. Furthermore, all six polyanions exhibited antiproliferative potency against A549 (non-small cell lung cancer), CH1/PA-1 (ovarian teratocarcinoma), and SW480 (colon carcinoma) cells, but it was higher for **1-P**, **1-As** , and **1-Ge** than for the phenyl–analogues **2-P**, **2-As**, and **2-Ge**. The activity of all six polyanions is specific against tumor cells, sincebecause a lowerweaker cytotoxic effect was observed in the HFF-1 cell line. The reason for the different bioactivity between the (*p*-tolyl)Sb-containing polyanions **1-P**, **1-As** , and **1-Ge** and the isostructural PhSb-containing polyanions **2-P**, **2-As**, and **2-Ge** appears to be due to an increased lipophilic character bydue to methyl–functionalization of the phenyl group in the *para* position. Our work demonstrates an important step forward in the goal to synthesizeof synthesizing polyanions with improved bioactivity and to unravelunraveling their mechanism of action.

Supporting Information

Supporting Information

Synthesis of (The Supporting pInformation tolyl)$SbCl_2$; FT-IR spectra (Figures S1-3); TGA thermograms (Figure S4); ^{1}H (Figure S6), and ^{13}C NMR spectra (Figure S5), as well as time-dependent ^{1}H NMR spectra (Figure S7). Early/late apoptosis and necrosis induction after 24 h in SW480 cells, analyzed by flow cytometry and averaged over three independent experiments (Figure S8). Tables with the main crystallographic and refinement parameters (Tables S1−S3), as well as MIC determination of the polyanions against the growth of bacteria (Table S4). Percentages of early/late apoptosis and necrosis induction by the investigated polyanions **1-P** , **1-As** , **1-Ge** , **2-P** , **2-As** and **2-Ge** in SW480 cells after exposure for 24 h (Table S5). This material is available free of charge *via* the Internet at http://pubs.acs.org https://pubs.acs.org/doi/10.1021/acs.inorgchem.9b03322 .

Synthesis of (*p*-tolyl)$SbCl_2$; FT-IR spectra (Figures S1–S3); TGA thermograms (Figure S4); ^{1}H (Figure S6) and ^{13}C NMR (Figure S5) spectra and time-dependent ^{1}H NMR spectra (Figure S7); early/late apoptosis and necrosis induction after 24 h in SW480 cells, analyzed by flow cytometry and averaged over three independent experiments (Figure S8); tables of the main crystallographic and refinement parameters (Tables S1–S3) and MICs of the polyanions against the growth of bacteria (Table S4); and percentages of early/late apoptosis and necrosis induction by the investigated polyanions **1-P**, **1-As**, **1-Ge**, **2-P**, **2-As**, and **2-Ge** in SW480 cells after exposure for 24 h (Table S5) (PDF)

Accession Codes

CCDC 1965371–1965373 contain the supplementary crystallographic data for this paper. These data can be obtained free of charge via www.ccdc.cam.ac.uk/data_request/cif, or by emailing data_request@ccdc.cam.ac.uk, or by contacting The Cambridge Crystallographic Data Centre, 12 Union Road, Cambridge CB2 1EZ, UK; fax: +44 1223 336033.

Notes

The authors declare no competing financial interest.

Acknowledgments

U.K. thanks the German Science Foundation (DFG-KO-2288/20-1 and DFG-KO-2288/26-1) and Jacobs University for research support. T.M. and P.Y. acknowledge the China Scholarship Council (CSC) for a doctoral fellowship. Z.L. thanks the National Natural Science Foundation of China (21701010) for research support. F.A., R.M., and C.S. greatlygratefully acknowledge the financial support from the National Research Council (CNCS) of Romania, through Research Project No. PN-II-ID-PCE-2011-3-0933. U.K. also acknowledges CMST COST Action CM1203 (PoCheMoN). Figure 1 was generated with Diamond, version 3.2 (copyright Crystal Impact GbR).

References

(1) (a) Pope, M. T. *Heteropoly and Isopoly Oxometalates*; Springer–Verlag: Berlin, 1983. (b) Barras-Almenar, J. J. ; Coronado, E. ; MüllerMüller, A. ; Pope, M. T. *Polyoxometalate Molecular Science*; Kluwer Academic Publishers: Dordrecht, The Netherlands, 2004. (c) Pope, M. T. ; Kortz, U. Polyoxometalates. In *Encyclopedia of Inorganic and Bioinorganic Chemistry*; John Wiley, 2012.

(2) (a) Mayer, C. R.; Thouvenot, R. Organophosphoryl derivatives of trivacant tungstophosphates of general formula α-A-$[PW_9O_{34}(RPO)_2]^{5-}$: synthesis and structure determination by multinuclear magnetic resonance spectroscopy (^{31}P, ^{183}W). *J. Chem. Soc., Dalton Trans.* **1998**, *1*, 7–1410.1039/a705216b. (b) Sun, Z.-G.; Liu, Q.; Liu, J.-F. Synthesis and spectroscopic characterization of organophosphoryl polyoxotungstates $[C_6H_{11}P(O)]_2X^{n+}W_{11}O_{39}^{(8-n)-}$ (X^{n+}=P^{5+},

Si^{4+}, B^{3+}, Ga^{3+}). *Polyhedron* **2000**, *19*, 125–128 10.1016/S0277-5387(99)00326-5. (c) Sun, Z.-G.; Liu, Q.; Liu, J.-F. Organophosphoryl polyoxotungstates α-$[R_2PW_9O_{34}]^{5-}$ [R = PhP(S), $C_6H_{11}P(O)$, $H_2NCH(n\text{-}Pr)P(O)$]. *Transition ~~Metal Chemistry~~Met. Chem.* **2000**, *25*, 374–376 10.1023/A:1007049514031. (d) Sun, Z.-G.; Zhang, L.-C.; Liu, Z.-M.; Cui, L.-Y.; Tian, C.-H.; Liang, H.-D.; Zhu, Z.-M.; You, W.-S. Synthesis, spectroscopic properties and crystal structure of organophosphoryl polyoxotungstate α-$[Bu_4N]_3H[PhCH_2P(O)]_2SiW_{11}O_{39}$. *J. Coord. Chem.* **2006**, *59*, 1557–1564 10.1080/00958970600561423. (e) Carraro, M.; Modugno, G.; Sartorel, A.; Scorrano, G.; Bonchio, M. Optically Active Polyoxotungstates Bearing Chiral Organophosphonate Substituents. *Eur. J. Inorg. Chem.* **2009**, *~~34~~2009*, 5164–5174 10.1002/ejic.200900728.

(3) (a) Mayer, C. R.; Cabuil, V.; Lalot, T.; Thouvenot, R. Incorporation of Magnetic Nanoparticles in New Hybrid Networks Based on Heteropolyanions and Polyacrylamide. *Angew. Chem., Int. Ed.* **1999**, *38*, 3672–3675 10.1002/(SICI)1521-3773(19991216)38:24<3672::AID-ANIE3672>3.0.CO;2-#. (b) Mayer, C. R.; Lalot, T.; Thouvenot, R. Hybrid Hydrogels Obtained by the Copolymerization of Acrylamide with Aggregates of Methacryloyl Derivatives of Polyoxotungstates. A Comparison with Polyacrylamide Hydrogels with Trapped Aggregates. *Macromolecules~~.~~* **2000**, *33*, 4433–4437 10.1021/ma991918h. (c) Niu, J.-Y.; Li, M.-X.; Wang, J.-P. Organosilyl derivatives of trivacant tungstophosphate of general formula α-A-$[PW_9O_{34}(RSiO)_3(RSi)]^{3-}$: Synthesis and structure determination by X-ray crystallography. *J. Organomet. Chem.* **2003**, *675*, 84–90 10.1016/S0022-328X(03)00252-3. (d) Mayer, C. R.; Roch-Marchal, C.; Lavanant, H.; Thouvenot, R.; Sellier, N.; Blais, J. C.; Secheresse, F. New Organosilyl Derivatives of the Dawson Polyoxometalate $[\alpha_2\text{-}P_2W_{17}O_{61}(RSi)_2O]^{6-}$: Synthesis and Mass Spectrometric Investigation. *Chem. - Eur. J. ~~Chem.~~* **2004**, *10*, 5517–5523 10.1002/chem.200400217. (e) Kato, C. N.; Kasahara, Y.; Hayashi, K.; Yamaguchi, A.; Hasegawa, T.; Nomiya, K. Syntheses, Characterization, and X-ray Crystal Structures of Mono-Lacunary Dawson Polyoxometalate-Based Organosilyl Complexes. *Eur. J. Inorg. Chem.* **2006**, *~~23~~2006*, 4834–4842 10.1002/ejic.200600479. (f) Proust, A.; Thouvenot, R.; Gouzerh, P. Functionalization of polyoxometalates: towards advanced applications in catalysis and materials science. *Chem. Commun.* **2008**, *16*, 1837–1852 10.1039/b715502f. (g) Zhang, T.; Mazaud, L.; Chamoreau, L.-M.; Paris, C.; Proust, A.; Guillemot, G. Unveiling the Active Surface Sites in Heterogeneous Titanium-Based Silicalite Epoxidation Catalysts: Input of Silanol-Functionalized Polyoxotungstates as Soluble Analogues. *ACS Catal.* **2018**, *8*, 2330–2342 10.1021/acscatal.8b00256.

(4) (a) Knoth, W. H. Derivatives of heteropolyanions. 1. Organic derivatives of $W_{12}SiO_{40}^{4-}$, $W_{12}PO_{40}^{3-}$, and $Mo_{12}SiO_{40}^{4-}$. *J. Am. Chem. Soc.* **1979**, *101*, 759–760 10.1021/ja00497a057. (b) Knoth, W. H. Derivatives of heteropolyanions. 2. Metal-metal-bonded derivatives. *J. Am. Chem. Soc.* **1979**, *101*, 2211–2213 10.1021/ja00502a052. (c) Zonnevijlle, F.; Pope, M. T. Attachment of organic groups to heteropoly oxometalate anions. *J. Am. Chem. Soc.* **1979**, *101*, 2731–2732 10.1021/ja00504a040. (d) Sazani, G.; Pope, M. T. Organotin and organogermanium linkers for simple, direct functionalization of polyoxotungstates. *Dalton Trans.* **2004**, *0*, 1989–1994 10.1039/b402421d. (e) Joo, N.; Renaudineau, S.; Delapierre, G.; Bidan, G.; Chamoreau, L.-M.; Thouvenot, R.; Gouzerh, P.; Proust, A. Organosilyl/-germyl Polyoxotungstate Hybrids for Covalent Grafting onto Silicon Surfaces: Towards Molecular Memories. *Chem. - Eur. J.* **2010**, *16*, 5043–5051 10.1002/chem.200903336. (f) Nomiya, K.; Togashi, Y.; Kasahara, Y.; Aoki, S.; Seki, H.; Noguchi, M.; Yoshida, S. Synthesis and Structure of Dawson Polyoxometalate-Based, Multifunctional, Inorganic–Organic Hybrid Compounds: Organogermyl Complexes with One Terminal Functional Group and Organosilyl Analogues with Two Terminal Functional Groups. *Inorg. Chem.* **2011**, *50*, 9606–9619 10.1021/ic201336v.

(5) (a) Artero, V.; Proust, A.; Herson, P.; Villain, F.; Cartier dit Moulin, C. ~~C. d.;~~ Gouzerh, P. Synthesis and characterization of the first carbene derivative of a polyoxometalate. *J. Am. Chem. Soc.* **2003**, *125*, 11156–11157 10.1021/ja036257p. (b) Laurencin, D.; Villanneau, R.; Herson, P.; Thouvenot, R.; Jeannin, Y.; Proust, A. Proust, A. A new organometallic heteropolytungstate related to $[Sb_2W_{22}O_{74}(OH)_2]^{12-}$: synthesis and structural characterisation of the bis-{Ru(*p*-cymene)}$^{2+}$-containing anion $[Sb_2W_{20}O_{70}\{Ru(p\text{-cymene})\}_2]^{10-}$. *Chem. Commun.* **2005**, 5524–5526 10.1039/b510300b. (c) Bi, L.-H.; Kortz, U.; Dickman, M. H.; Keita, B.; Nadjo, L. Trilacunary Heteropolytungstates Functionalized by Organometallic Ruthenium(II), $[(RuC_6H_6)_2XW_9O_{34}]^{6-}$ (X = Si, Ge). *Inorg. Chem.* **2005**, *44*, 7485–7493 10.1021/ic0508627. (d) Sadakane, M.; Iimuro, Y.; Tsukuma, D.; Bassil, B. S.; Dickman, M. H.; Kortz, U.; Zhang, Y.; Ye, S.; Ueda, W. Carbonyl–ruthenium substituted α-Keggin-tungstosilicate, $[\alpha\text{-}SiW_{11}O_{39}Ru^{II}(CO)]^{6-}$: synthesis, structure, redox studies and reactivity. *Dalton Trans.* **2008**, 6692–6698 10.1039/b810987g. (e) Meng, R.-Q.; Suo, L.; Hou, G.-F.; Liang, J.; Bi, L.-H.; Li, H.-L.; Wu, L.-X.

Organo-Ru supported sandwich-type tungstoarsenates: Synthesis, structure and catalytic properties. *CrystEngComm* **2013**, *15*, 5867–5876 10.1039/c3ce00045a. (f) Abramov, P. A.; Sokolov, M. N.; Floquet, S.; Haouas, M.; Taulelle, F.; Cadot, E.; Peresypkina, E. V.; Virovets, A. V.; Vicent, C.; Kompankov, N. B.; Zhdanov, A. A.; Shuvaeva, O. V.; Fedin, V. P. Coordination-Induced Condensation of $[Ta_6O_{19}]^{8-}$: Synthesis and Structure of $[\{(C_6H_6)Ru\}_2Ta_6O_{19}]^{4-}$ and $[\{(C_6H_6)RuTa_6O_{18}\}_2(\mu\text{-}O)]^{10-}$. *Inorg. Chem.* **2014**, *53*, 12791–12798 10.1021/ic501622t.
(6) (a) Knoth, W. H.; Harlow, R. L. Derivatives of heteropolyanions. 3. O-alkylation of $Mo_{12}PO_{40}^{3-}$ and $W_{12}PO_{40}^{3-}$. *J. Am. Chem. Soc.* **1981**, *103*, 4265–4266 10.1021/ja00404a056. (b) Bareyt, S.; Piligkos, S.; Hasenknopf, B.; Gouzerh, P.; ~~Lacôte~~Lacôte, E.; Thorimbert, S.; Malacria, M. Highly Efficient Peptide Bond Formation to Functionalized Wells-Dawson-Type Polyoxotungstates. *Angew. Chem., Int. Ed.* **2003**, *42*, 3404–3406 10.1002/anie.200351346. (c) Kortz, U.; Hussain, F.; Reicke, M. The Ball-Shaped Heteropolytungstates $[\{Sn(CH_3)_2(H_2O)\}_{24}\{Sn(CH_3)_2\}_{12}(A\text{-}XW_9O_{34})_{12}]^{36-}$. *Angew. Chem., Int. Ed.* **2005**, *44*, 3773–3777 10.1002/anie.200500548. (d) Izzet, G.; ~~Ménand~~Ménand, M.; Matt, B.; Renaudineau, S.; Chamoreau, L.-M.; Sollogoub, M.; Proust, A. Cyclodextrin-Induced Auto-Healing of Hybrid Polyoxometalates. *Angew. Chem., Int. Ed.* **2012**, *51*, 487–490 10.1002/anie.201106727. (e) Sang, X.-J.; Li, J.-S.; Zhang, L.-C.; Zhu, Z.-M.; Chen, W.-L.; Li, Y.-G.; Su, Z.-M.; Wang, E.-B. Two carboxyethyltin functionalized polyoxometalates for assembly on carbon nanotubes as efficient counter electrode materials in dye-sensitized solar cells. *Chem. Commun.* **2014**, *50*, 14678–14681 10.1039/C4CC06211F. (f) Han, Q.; Liu, J.-C.; Wen, Y.; Chen, L.-J.; Zhao, J.-W.; Yang, G.-Y. Tellurotungstate-based organotin–rare-earth heterometallic hybrids with four organic components. *Inorg. Chem.* **2017**, *56*, 7257–7269 10.1021/acs.inorgchem.7b00924.
(7) (a) Pope, M. T. ; ~~Müller~~Müller, A. *Polyoxometalate: from Platonic Solids to Antiviral Activity*; Kluwer Academic Publishers: Dordrecht, The Netherlands, 1994. (b) Gouzerh, P.; Proust, A. Main-group element, organic, and organometallic derivatives of polyoxometalates. *Chem. Rev.* **1998**, *98*, 77–111 10.1021/cr960393d. (c) Rhule, J. T.; Hill, C. L.; Judd, D. A.; Schinazi, R. F. Polyoxometalates in medicine. *Chem. Rev.* **1998**, *98*, 327–358 10.1021/cr960396q. (d) Dolbecq, A.; Dumas, E.; Mayer, C. R.; Mialane, P. Hybrid organic–inorganic polyoxometalate compounds: from structural diversity to applications. *Chem. Rev.* **2010**, *110*, 6009–6048 10.1021/cr1000578. (e) Bijelic, A.; Rompel, A. The use of polyoxometalates in protein crystallography–An attempt to widen a well-known bottleneck. *Coord. Chem. Rev.* **2015**, *299*, 22–38 10.1016/j.ccr.2015.03.018. (f) Bijelic, A.; Aureliano, M.; Rompel, A. Polyoxometalates as potential next-generation metallodrugs in the combat against cancer. *Angew. Chem., Int. Ed.* ~~**2018**~~**2019**, ~~*57*~~*58*, ~~22980–22~~22999 10.1002/anie.201803868. (g) Bijelic, A.; Aureliano, M.; Rompel, A. The antibacterial activity of polyoxometalates: structures, antibiotic effects and future perspectives. *Chem. Commun.* **2018**, *54*, 1153–1169 10.1039/C7CC07549A. (h) ~~Čolović~~Čolović, M.; ~~Lacković~~Lacković, M.; ~~Lalatović~~Lalatović, J.; Mougharbel, A. S.; Kortz, U.; ~~Krstić~~Krstić, D. Z. Polyoxometalates in Biomedicine: Update and Overview. *Curr. Med. Chem.* ~~**2020**~~**2019**, 10.2174/0929867326666190827153532. (i) Yang, P.; Ma, T.; Lang, Z.-L.; Misirlic-Dencic, S.; ~~Isaković~~Isaković, A. M.; ~~Bényei~~Bényei, A.; ~~Čolović~~Čolović, M. B.; Markovic, I.; ~~Krstić~~Krstić, D. Z.; Poblet, J. M.; Lin, Z.-G.; Kortz, U. Tetravalent Metal Ion Guests in Polyoxopalladate Chemistry: Synthesis and Anticancer Activity of $[MO_8Pd_{12}(PO_4)_8]^{12-}$ (M = Sn^{IV}, Pb^{IV}). *Inorg. Chem.* **2019**, *58*, 11294–11299 10.1021/acs.inorgchem.9b01129. (j) Gott, M.; Yang, P.; Kortz, U.; Stephan, H.; Pietzsch, H.-J.; Mamat, C. A 224 Ra-labeled polyoxopalladate as a putative radiopharmaceutical. *Chem. Commun.* **2019**, *55*, 7631–7634 10.1039/C9CC02587A. (k) Francese, R.; Civra, A.; ~~Ritta~~Ritta, M.; Donalisio, M.; Argenziano, M.; Cavalli, R.; Mougharbel, A. S.; Kortz, U.; Lembo, D. Anti-zika virus activity of polyoxometalates. ~~*Antivir.*~~*Antiviral Res.* **2019**, *163*, 29–33 10.1016/j.antiviral.2019.01.005.
(8) Huang, Y.-Z. Synthetic applications of organoantimony compounds. *Acc. Chem. Res.* **1992**, *25*, 182–187 10.1021/ar00016a002.
(9) Haiduc, I.; Silvestru, C. Metal compounds in cancer chemotherapy. *Coord. Chem. Rev.* **1990**, *99*, 253–296 10.1016/0010-8545(90)80065-2.
(10) (a) Silvestru, C.; Haiduc, I. Structural patterns in inorganic and organoantimony derivatives of oxo-and thiodiorganophosphorus ligands. *Coord. Chem. Rev.* **1996**, *147*, 117–146 10.1016/0010-8545(95)01129-3. (b) Prabhu, M. S. R.; Jami, A. K.; Baskar, V. Organoantimony(V) Oxido Cubane Cluster $[(p\text{-}X\text{-}C_6H_4Sb)_4(O)_4(Ph_2SiO_2)_4]$ (X = Cl, Br) Stabilized by Diphenyldisiloxides. *Organometallics* **2009**, *28*, 3953–3956 10.1021/om900244t. (c) Nicholson, B. K.; Clark, C. J.; Wright, C. E.; Groutso, T. Isopolyoxometalates of Antimony: Arylstibonic Acids $[H_8(RSb)_{12}O_{28}]$ and Derived Dodecanuclear Polyoxostibonates $[M_2H_{10-x}(RSb)_{12}O_{30}]^{x-}$, M = Na or K. *Organometallics* **2010**, *29*, 6518–6526 10.1021/om1008692. (d) Jami, A. K.; Prabhu, M. S. R.; Baskar, V. Isolation

of tetranuclear organoantimony oxo clusters and hexa-decanuclear polyoxostibonates. *Organometallics* **2010**, *29*, 1137–114310.1021/om900942q. (e) Nicholson, B. K.; Clark, C. J.; Wright, C. E.; Telfer, S. G.; Groutso, T. New Sb_{12} and Sb_{14} Polyoxometalate Frameworks Derived from Arylstibonic Acids: $[LiH_3(p\text{-}MeC_6H_4Sb)_{12}O_{28}]^{4-}$ and $[BaH_{10}(p\text{-}MeC_6H_4Sb)_{14}O_{34}]$. *Organometallics* **2011**, *30*, 6612–661610.1021/om200739a.
(11) Barsukova-Stuckart, M.; Piedra-Garza, L. F.; Gautam, B.; Alfaro-Espinoza, G.; Izarova, N. V.; Banerjee, A.; Bassil, B. S.; Ullrich, M. S.; Breunig, H. J.; Silvestru, C.; Kortz, U. Synthesis and biological activity of organoantimony (III)-containing heteropolytungstates. *Inorg. Chem.* **2012**, *51*, 12015–12022 10.1021/ic301892s.
(12) (a) Yang, P.; Bassil, B. S.; Lin, Z.; Haider, A.; Alfaro-Espinoza, G.; Ullrich, M. S.; Silvestru, C.; Kortz, U. Organoantimony (III)-Containing Tungstoarsenates (III): From Controlled Assembly to Biological Activity. *Chem. - Eur. J.* **2015**, *21*, 15600–15606 10.1002/chem.201502398. (b) Yang, P.; Lin, Z.; Alfaro-Espinoza, G.; Ullrich, M. S.; Rat, C. I.; Silvestru, C.; Kortz, U. 19-Tungstodiarsenate (III) Functionalized by Organoantimony (III) Groups: Tuning the Structure–Bioactivity Relationship. *Inorg. Chem.* **2016**, *55*, 251–258 10.1021/acs.inorgchem.5b02189. (c) Yang, P.; Lin, Z.; Bassil, B. S.; Alfaro-Espinoza, G.; Ullrich, M. S.; Li, M.-X.; Silvestru, C.; Kortz, U. Tetra-Antimony(III)-Bridged 18-Tungsto-2-Arsenates(V), $[(LSb^{III})_4(A\text{-}\alpha\text{-}As^{V}W_9O_{34})_2]^{10-}$ (L = Ph, OH): Turning Bioactivity On and Off by Ligand Substitution. *Inorg. Chem.* **2016**, *55*, 3718–3720 10.1021/acs.inorgchem.6b00107.
(13) (a) Liu, B.-Y.; Ku, Y.-T.; Wang, M.; Wang, B.-Y.; Zheng, P.-J. A New Type of Organostibonic Molybdate. Synthesis and Structure of a Tetra-n-butylammonium Salt of Diphenylstibonomolybdate. *J. Chem. Soc., Chem. Commun.* **1989**, 651–652 10.1039/c39890000651. (b) Piedra-Garza, L. F.; Dickman, M. H.; Moldovan, O.; Breunig, H. J.; Kortz, U. Organoantimony-Containing Polyoxometalate: $[\{PhSbOH\}_3(A\text{-}\alpha\text{-}PW_9O_{34})_2]^{9-}$. *Inorg. Chem.* **2009**, *48*, 411–413 10.1021/ic8021694.
(14) (a) Domaille, P. J. Potassium octadecatungstodiphophates (V) and related lacunary compounds. *Inorg. Synth.* **1990**, *27*, 100. (b) Contant, R.; Thouvenot, R.; Dromzee, Y.; Proust, A.; Gouzerh, P. Synthesis and structural chemistry of tungstoarsenates (V). *J. Cluster Sci.* **2006**, *17*, 317–331 10.1007/s10876-006-0054-0. (c) Herve, G.; Teze, A. Study of. alpha.-and. beta.-enneatungstosilicates and-germanates. *Inorg. Chem.* **1977**, *16*, 2115–2117 10.1021/ic50174a060.
(15) (a) Talalaeva, ~~T.V~~T. V.; Kocheshkov, K. A. Synthesis of antimony organic compounds by lithium organic compounds. *Russ. J. Gen. Chem.* **1946**, *16*, 777–780. (b) Nunn, M.; Sowerby, ~~D.B~~D. B.; Wesolek, ~~D.M~~D. M. The preparation of phenyl substituted antimony (III) and antimony (V) chlorides and bromides. *J. Organomet. Chem.* **1983**, *251*, C45–C46 10.1016/S0022-328X(00)98787-4. (c) Millington, P. L.; Sowerby, D. B. Preparation and crystal structures of five organoantimony halides; (*p*-tolyl)antimony(III) dichloride and dibromide, diphenylantimony(III) bromide, 2′-diyl)antimony(III) chloride and bis-(2′-chlorobiphenyl-2-yl)antimony(V) trichloride. *J. Organomet. Chem.* **1994**, *480*, 227–234 10.1016/0022-328X(94)87123-X.
(16) Sheldrick, G. M. *SADABS, Program for empirical X-ray absorption correction*; ~~Bruker-Nonius~~ Bruker-Nonius : ~~Madison, WI~~ Madison, WI , 1990.
(17) Sheldrick, G. M. A Short History of SHELX. *Acta Crystallogr., Sect. A: Found. Crystallogr.* **2008**, *A64*, 112–122 10.1107/S0108767307043930.
(18) Vezzulli, L.; Grande, C.; Reid, P. C.; ~~Hélaouët~~Hélaouët, P.; Edwards, M.; ~~Höfle~~Höfle, M. G.; Brettar, I.; Colwell, R. R.; Pruzzo, C. Climate influence on Vibrio and associated human diseases during the past half-century in the coastal North Atlantic. *Proc. Natl. Acad. Sci. U. S. A.* **2016**, *113*, ~~e5062~~E5062 ~~e5071~~E5071 10.1073/pnas.1609157113.
(19) Cavalli, R.; Donalisio, M.; Bisazza, A.; Civra, A.; Ranucci, E.; Ferruti, P.; Lembo, D. Enhanced antiviral activity of acyclovir loaded into nanoparticles. *Methods Enzymol.* **2012**, *509*, 1–19 10.1016/B978-0-12-391858-1.00001-0.
(20) Brown, I. D.; Altermatt, D. Bond-valence parameters obtained from a systematic analysis of the inorganic crystal structure database. *Acta Crystallogr., Sect. B: Struct. Sci.* **1985**, *41*, 244–247 10.1107/S0108768185002063.
(21) Mukherjee, H. N. ~~TREATMENT OF CANCER OF THE INTESTINAL TRACT WITH A COMPLEX COMPOUND OF PHOSPHOTUNGSTIC PHOSPHOMOLYBDIC ACIDS AND CAFFEINE~~Treatment of cancer of the intestinal tract with a complex compound of phosphotungstic phosphomolybdic acids and caffeine. *J. Indian Med. Assoc.* **1965**, *44*, 477–479.